

# Diode-pumped multi-frequency Q-switched laser with intracavity cascade Raman emission

Y. T. Chang, Y. P. Huang, K. W. Su, and Y. F. Chen\*

Department of Electrophysics, National Chiao Tung University, Hsinchu, Taiwan  
[yfchen@cc.nctu.edu.tw](mailto:yfchen@cc.nctu.edu.tw)

**Abstract:** A diode-pumped actively Q-switched mixed Nd:Y<sub>0.3</sub>Gd<sub>0.7</sub>VO<sub>4</sub> laser with an intracavity KTP crystal is developed to produce cascade SRS emission up to the fourth order. With an incident pump power of 14 W and a repetition rate of 50 kHz, the average output powers at the first, second, third and fourth Stokes modes are approximately 0.05 W, 0.61 W, 0.25 W, and 0.11 W, respectively. The maximum peak power is greater than 2 kW.

©2008 Optical Society of America

OCIS codes: (140.3540) Lasers, Q-switched (140.3550) Lasers, Raman.

## References and links

1. R. A. Fields, M. Birnbaum, and C. L. Fincher, "Highly efficient Nd:YVO<sub>4</sub> diode-laser end-pumped laser," *Appl. Phys. Lett.* **51**, 1885-1886 (1987).
2. A. Sennaroglu, "Efficient continuous-wave operation of a diode-pumped Nd:YVO<sub>4</sub> laser at 1342 nm," *Opt. Commun.* **164**, 191-197 (1999).
3. Y. F. Chen, "Design criteria for concentration optimization in scaling diode end-pumped lasers to high powers: influence of thermal fracture," *IEEE J. Quantum Electron.* **35**, 234-239 (1999).
4. A. Y. Yao, W. Hou, Y. P. Kong, L. Guo, L. A. Wu, R. N. Li, D. F. Cui, Z. Y. Xu, Y. Bi, and Y. Zhou, "Double-end-pumped 11-W Nd:YVO<sub>4</sub> cw laser at 1342 nm," *J. Opt. Soc. Am. B* **22**, 2129-2133 (2005).
5. T. Jensen, V. G. Ostroumov, J. P. Meyn, G. Huber, A. I. Zagumennyi, and I. A. Shcherbarkov, "Spectroscopic characterization and laser performance of diode-laser-pumped Nd:GdVO<sub>4</sub>," *Appl. Phys. B* **58**, 373-379 (1994).
6. H. J. Zhang, X. L. Meng, L. Zhu, H. Z. Zhang, P. Wang, J. Dawes, C. Q. Wang, and Y. T. Chow, "Investigation on the growth and laser properties of Nd:GdVO<sub>4</sub> single crystal," *Cryst. Res. Technol.* **33**, 801-806 (1998).
7. T. Ogawa, Y. Urata, S. Wada, K. Onodera, H. Machida, H. Sagae, M. Higuchi, and K. Kodaira, "Efficient laser performance of Nd:GdVO<sub>4</sub> crystals grown by the floating zone method," *Opt. Lett.* **28**, 2333-2335 (2003).
8. V. Lupei, N. Pavel, Y. Sato, and T. Taira, "Highly efficient 1063-nm continuous-wave laser emission in Nd:GdVO<sub>4</sub>," *Opt. Lett.* **28**, 2366-2368 (2003).
9. L. J. Qin, X. L. Meng, L. Zhu, J. H. Liu, B. C. Xu, H. Z. Xu, F. Y. Jiang, C. L. Du, X. Q. Wang, and Z. S. Shao, "Influence of the different Gd/Y ratio on the properties of Nd:Y<sub>x</sub>Gd<sub>1-x</sub>VO<sub>4</sub> mixed crystals," *Chem. Phys. Lett.* **380**, 273-278 (2003).
10. J. Liu, X. Meng, Z. Shao, M. Jiang, B. Ozygus, A. Ding, and H. Weber, "Pulse energy enhancement in passive Q-switching operation with a class of Nd:Gd<sub>x</sub>Y<sub>1-x</sub>VO<sub>4</sub> crystals," *Appl. Phys. Lett.* **83**, 1289-1291 (2003).
11. Y. F. Chen, M. L. Ku, L. Y. Tsai, and Y. C. Chen, "Diode-pumped passively Q-switched picosecond Nd:Gd<sub>x</sub>Y<sub>1-x</sub>VO<sub>4</sub> self-stimulated Raman laser," *Opt. Lett.* **29**, 2279-2281 (2004).
12. J. L. He, Y. X. Fan, J. Du, Y. G. Wang, S. Liu, H. T. Wang, L. H. Zhang, and Y. Hang, "4-ps passively mode-locked Nd:Gd<sub>0.5</sub>Y<sub>0.5</sub>VO<sub>4</sub> laser with a semiconductor saturable-absorber mirror," *Opt. Lett.* **29**, 2803-2805 (2004).
13. S. P. Ng, D. Y. Tang, A. Q. Liu, L. J. Qin, and X. L. Meng, "Short pulse passively Q-switched NdGdYVO<sub>4</sub> laser using a GaAs mirror," *Opt. Commun.* **259**, 256-260 (2006).
14. H. H. Yu, H. J. Zhang, Z. P. Wang, J. Y. Wang, Y. G. Yu, Z. S. Shao, M. H. Jiang, and X. Y. Zhang, "Continuous wave and passively Q-switched laser performance of Nd-doped mixed crystal Nd:Lu<sub>0.5</sub>Gd<sub>0.5</sub>VO<sub>4</sub>," *Appl. Phys. Lett.* **90**, 231110 (2007).
15. A. A. Kaminskii, "Modern developments in the physics of crystalline laser materials," *Phys. Status Solidi (A)* **200**, 215-296 (2003).
16. T. T. Basiev and R. C. Powell, "Special issue on solid state Raman lasers-Introduction," *Opt. Mater.* **11**, 301-306 (1999).
17. H. M. Pask, "The design and operation of solid-state Raman lasers," *Prog. Quantum Electron.* **27**, 3-56 (2003).
18. Y. F. Chen, "Stimulated Raman scattering in a potassium titanyl phosphate crystal: simultaneous self-sum frequency mixing and self-frequency doubling," *Opt. Lett.* **30**, 400-402 (2005).

19. S. Pearce, C. L. M. Ireland, and P. E. Dyer, "Solid-state Raman laser generating <1ns, multi-kilohertz pulses at 1096 nm," *Opt. Commun.* **260**, 680-686 (2006).
20. V. Pasiskevicius, C. Canalias, and F. Laurell, "Highly efficient stimulated Raman scattering of picosecond pulses in KTiOPO<sub>4</sub>," *Appl. Phys. Lett.* **88**, 041110 (2006).
21. G. A. Massey, T. M. Loehr, L. J. Willis, and J. C. Johnson, "Raman and Electro-optic Properties of Potassium Titanate Phosphate," *Appl. Opt.* **19**, 4136-4137 (1980).
22. K. Kawase, M. Mizuno, S. Sohma, H. Takahashi, T. Taniuchi, Y. Urata, S. Wada, H. Tashiro, and H. Ito, "Difference-frequency terahertz-wave generation from 4-dimethylamino-N-methyl-4-stilbazolium-tosylate by use of an electronically tuned Ti:sapphire laser," *Opt. Lett.* **24**, 1065-1067 (1999).
23. K. Kawase, T. Hatanaka, H. Takahashi, K. Nakamura, T. Taniuchi, and H. Ito, "Tunable terahertz-wave generation from DAST crystal by dual signal-wave parametric oscillation of periodically poled lithium niobate," *Opt. Lett.* **25**, 1714-1716 (2000).
24. K. Suizu, K. Miyamoto, T. Yamashita, and H. Ito, "High-power terahertz-wave generation using DAST crystal and detection using mid-infrared powermeter," *Opt. Lett.* **32**, 2885-2887 (2007).
25. J. J. Zayhowski and A. Mooradian, "Single-frequency microchip Nd lasers," *Opt. Lett.* **14**, 24-26 (1989).
26. G. J. Dixon, L. S. Lingvay, and R. H. Jarman, "Properties of close coupled monolithic, lithium neodymium, tetraphosphate lasers," *Proc. SPIE* **1104**, 107 (1989).
27. Y. F. Chen, T. M. Huang, C. F. Kao, C. L. Wang, and S. C. Huang, "Optimization in scaling fiber-coupled laser-diode end-pumped lasers to higher power: influence of thermal effect," *IEEE J. Quantum Electron.* **33**, 1424-1429 (1997).
28. Y. F. Chen, "High-power diode-pumped Q-switched intracavity frequency-doubled Nd:YVO<sub>4</sub> laser with a sandwich-type resonator," *Opt. Lett.* **24**, 1032-1034 (1999).

## 1. Introduction

Neodymium-doped single vanadate crystals including Nd:YVO<sub>4</sub> and Nd:GdVO<sub>4</sub> have been identified as excellent laser materials for diode-pumped solid-state lasers because of their large absorption and large emission cross sections [1-8]. In the Q-switching operation, however, the large emission cross sections usually limit their energy storage capacities. To overcome this hindrance, mixed Nd:Y<sub>x</sub>Gd<sub>1-x</sub>VO<sub>4</sub> crystals were recently developed with Y ions replacing some of the Gd ions in Nd:GdVO<sub>4</sub> single crystal [9-12]. It has been experimentally confirmed that such mixed crystals are substantially superior to single crystals for Q-switching and mode-locking performance because of their broader fluorescence linewidth [12-14].

Raman lasers which are based on intracavity stimulated Raman scattering (SRS) in Raman active crystals have a very promising potential for various applications such as pollution detection, remote sensing, and medical system [15-17]. Recently, potassium titanyl phosphate (KTP) and rubidium titanyl phosphate (RTP) which are widely recognized as prominent nonlinear optical crystals involving nonlinear optical susceptibility  $\chi^{(2)}$  have been experimentally confirmed to be practical SRS converter devices [18-20]. The low value of the KTP-related Stokes shift (270 cm<sup>-1</sup>) [21] permits generation of multi-frequency radiation with cascade SRS. Nowadays, simultaneous multi-frequency lasing lines with high peak powers in the room temperature is of practical importance for the terahertz (THz) generation with the nonlinear optical difference frequency method [22-24].

In this paper, we present the first demonstration of a diode-pumped actively Q-switched mixed Nd:Y<sub>0.3</sub>Gd<sub>0.7</sub>VO<sub>4</sub> laser with an intracavity KTP crystal to produce cascade SRS emission up to the fourth order. With an incident pump power of 14 W, the actively Q-switched intracavity Raman laser, operating at 50 kHz, produces an average output power up to 0.92 W with a pulse energy of 18.4 μJ. The maximum peak power is generally higher than 2 kW.

## 2. Experimental setup

The schematic diagram for the experimental setup of a diode-pumped actively Q-switched Nd:Y<sub>x</sub>Gd<sub>1-x</sub>VO<sub>4</sub> laser with a KTP crystal as an intracavity SRS medium is illustrated in Fig. 1. Spontaneous Raman spectral data on KTP crystal reveal that the strongest Raman scattering was observed near 270 cm<sup>-1</sup> [21]. With a fundamental pump wavelength of 1064 nm, the first four Stokes lines for the most intense Raman peak can be calculated to be 1096, 1129, 1166, and

1204 nm, respectively. The flat front mirror has antireflection coating ( $R < 0.2\%$ ) at the diode wavelength on the entrance face, high-reflection coating ( $R > 99.5\%$ ) at the lasing and SRS wavelengths, and high-transmission coating ( $T > 90\%$ ) at the diode wavelength on the other surface. The flat output coupler had the reflectivities  $R = 99.6\%$  at 1064 nm,  $R = 99.1\%$  at 1096 nm,  $R = 86.3\%$  at 1129 nm,  $R = 48.0\%$  at 1166 nm, and  $R = 27.5\%$  at 1204 nm. Note that the present output coupler was selected, but not optimized, from the available mirrors in our laboratory. Nevertheless, experimental results revealed that cascade SRS operation including the first four Stokes components could be obtained.

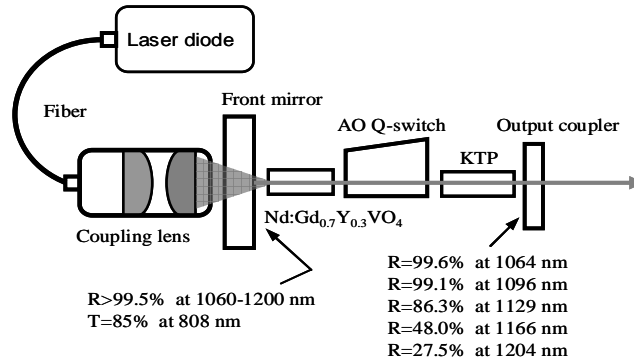


Fig. 1. Experimental setup for a diode-pumped actively Q-switched Nd:Y<sub>0.3</sub>Gd<sub>0.7</sub>VO<sub>4</sub> laser with a KTP crystal as an intracavity SRS medium.

The pump source was an 808-nm fiber-coupled laser diode (Coherent Inc.) with a core diameter of 0.8 mm, a numerical aperture of 0.16, and a maximum output power of 16 W. A focusing lens with a 12.5-mm focal length and 85% coupling efficiency was used to reimaged the pump beam into the laser crystal. The average radius of the pump beam was near 0.35 mm. The active laser medium was a 0.2-at.% Nd:Y<sub>0.3</sub>Gd<sub>0.7</sub>VO<sub>4</sub> crystal with a length of 10 mm. The Raman medium was a 20-mm-long KTP crystal with a cutting angle along the  $x$  axis ( $\theta = 90^\circ$  and  $\phi = 0^\circ$ ). Both sides of the Nd:Y<sub>0.3</sub>Gd<sub>0.7</sub>VO<sub>4</sub> and KTP crystals were coated for antireflection at 1000–1200 nm ( $R < 0.2\%$ ). In addition, they were wrapped with indium foil and mounted in a water-cooled copper block. The water temperature was maintained at 20 °C. The 30-mm-long acousto-optic Q-switch device (NEOS Model 33027-15-2-1) had antireflection coating at 1064 nm on both faces and was driven at a 27.12-MHz center frequency with 15.0 W of rf power.

The present cavity is a flat–flat resonator that was stabilized by the thermally induced lens in the laser crystal. This concept was found nearly simultaneously by Zayhowski and Mooradian [25] and by Dixon *et al* [26]. A linear flat–flat cavity is an attractive design because it reduces complexity and makes the system compact and rugged. However, the end-pump-induced thermal lens is not a perfect lens, but is rather a lens with aberration. It has been found that the thermally induced diffraction loss is a rapidly increasing function of the mode-to-pump ratio at a given pump power. When the incident pump power is greater than 5 W, the optimum mode-to-pump ratio is found to be in the range of 0.8-1.0 [27]. Since the laser rod is very close to the front mirror, the laser mode size in the gain medium can be given by [28]

$$\omega_t = \sqrt{\frac{\lambda}{\pi}} \frac{(L f_{th})^{1/4}}{(1 - L/f_{th})^{1/4}} \quad (1)$$

where  $f_{th}$  is the effective focal length of the thermal lens,

$$L = L_{cav} + l(1/n - 1) + l_{KTP}(1/n_{KTP} - 1) + l_Q(1/n_Q - 1) \quad (2)$$

is the effective cavity length,  $L_{cav}$  is the cavity length,  $l$  is the length of the gain medium,  $n$  is the refractive index of the gain medium,  $l_{KTP}$  is the length of the KTP crystal,  $n_{KTP}$  is the KTP refractive index for the output laser beam,  $l_Q$  is the length of the Q-switched crystal, and  $n_Q$  is the refractive index of the Q-switched crystal for the output laser beam. The effective focal length for an end-pumped laser rod can be approximately expressed as

$$f_{th} = C \omega_p^2 / P_{in} \quad (3)$$

where  $\omega_p$  is the pump size in the unit of mm,  $P_{in}$  is the incident pump power in the unit of watt (W), and  $C$  is a proportional constant in the unit of W/mm. The effective focal length at a given pump power can be experimentally estimated from the longest cavity length with which a flat-flat cavity can sustain stable. Therefore, we perform the laser experiments to obtain the critical cavity lengths for different pump powers at a fixed pump size. We used Eq. (3) to fit the experimental results and found the constant  $C$  to be approximately  $1.7 \times 10^4$  W/mm.

The dependence of the mode-to-pump size ratio on the pump power for the present cavity was calculated by using Eqs. (1)-(3) and the following parameters:  $C = 1.7 \times 10^4$  W/mm,  $\omega_p = 0.35$  mm,  $l_Q = 30$  mm,  $n_Q = 1.5$ ,  $l = 10$  mm,  $n = 2.16$ ,  $n_{KTP} = 1.75$ , and  $l_{KTP} = 20$  mm. The calculated results for several cavity lengths were shown in Fig. 2. It is clear that the mode-to-pump size ratio is around 0.8 at  $L_{cav} = 130$  mm for the pump powers in the range of 5~15 W, leading to a good compromise between overlapping efficiency and thermal effect. As a consequence, we arranged the cavity length to be 130 mm.

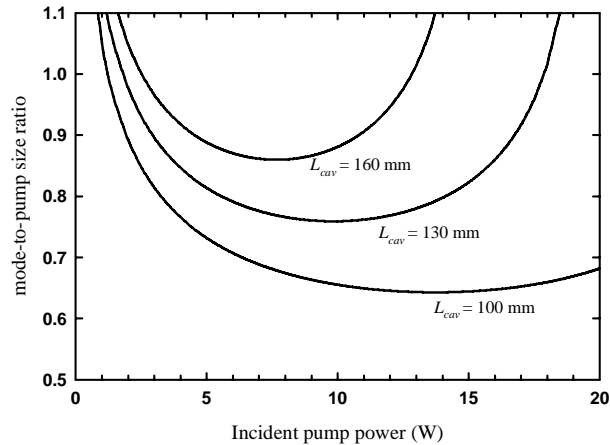


Fig. 2. Dependence of the mode-to-pump size ratio on the incident pump power for several cavity lengths.

### 3. Experimental results and discussions

Figure 3 depicts the average output powers with respect to the incident pump power at the 50-kHz Q-switching operation for the setup shown in Fig. 1. The threshold powers for the first Stokes mode is 4.5 W. The first Stokes output at 1096 nm increases with the pump power until the second Stokes threshold of 6.2 W is reached, and it is then clamped at a level of 50 mW. When the pump power is increased to approximately 8.2 W, the third Stokes radiation at 1166 nm start to be emitted and the second Stokes emission is almost saturated at a power of 0.6 W. The slope efficiency of the second Stokes at 1129 nm with respect to the pump power from 6.2 W to 8.2 W is approximately 30%. At pump power higher than the fourth Stokes

threshold of 10.5 W, the total output power is nearly clamped at 0.92 W. The maximum output powers at 1096 nm, 1129 nm, 1166 nm, and 1204 nm are approximately 0.05 W, 0.61 W, 0.25 W, and 0.11 W, respectively. Note that the present output coupler was not optimized for the overall conversion efficiency. Therefore, it is possible to obtain a higher output power with the optimum output coupler. On the other hand, the optimum conversion efficiency for the specific Stokes component can be obtained by optimizing the output coupler with high reflection for the lower order Stokes modes and high transmission for the next order Stokes mode. Furthermore, no damage to the KTP crystal was observed over several hours of operation, and the laser performance was reproducible on a day-to-day basis.

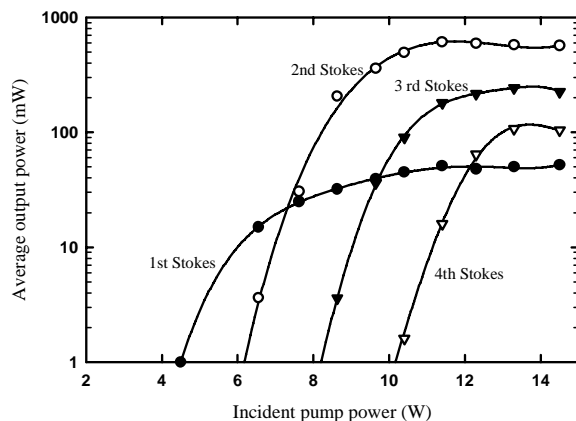


Fig. 3. Dependence of the average output power on the incident pump power for Q-switching operation at 50 kHz.

An optical spectrum analyzer (Advantest Q8381A) was used to measure the spectral information of the laser output. The present spectrum analyzer employing a diffraction lattice monochromator can be used for high-speed measurement of pulse light with a resolution of 0.1 nm. Figure 4 shows the emission spectrum measured at the output of the Raman laser for the pump power of 14.0 W. It can be seen that the optical spectra include the main output of the different order Stokes lines as well as the residual outputs of the fundamental wave at 1064 nm. The frequency shift between the Stokes and the laser lines is in good agreement with the asymmetric bending mode of a distorted  $\text{TiO}_6$  octahedron  $270 \text{ cm}^{-1}$  [21].

The temporal behavior of the output pulse was recorded by a LeCroy digital oscilloscope (Wavepro 7100, 1-GHz bandwidth, 10 G samples/sec) with two InGaAs p-i-n photodiodes for measuring the output pulses at fundamental and SRS emissions, respectively. The temporal characteristics of the fundamental pulse and Raman pulses are depicted in Figs. 5(a)-5(d) for four different pump powers of 5.0 W, 7.0 W, 9.0 W and 11.0 W. It can be seen that when the intracavity power density at the fundamental wavelength reaches the SRS threshold, the fundamental pulse is rapidly converted the Stokes output. Although the channel numbers of the oscilloscope are not sufficient to separate the temporal profiles of each Stokes orders, the experimental results in Figs. 5(a)-5(d) apparently reveal that various order Stokes pulses are generated step by step with increasing the pump power. Furthermore, the Q-switched pulse envelope displays clear modulated pulses. The separation of the modulated pulses was found to be 0.86 ns, which matched exactly with the cavity roundtrip time. Therefore, the modulated pulses can be confirmed to come from the longitudinal-mode beating. The estimated energy of the highest pulse inside envelope was found to be close to  $18.4 \mu\text{J}$  and the maximum peak power was greater than 2 kW.

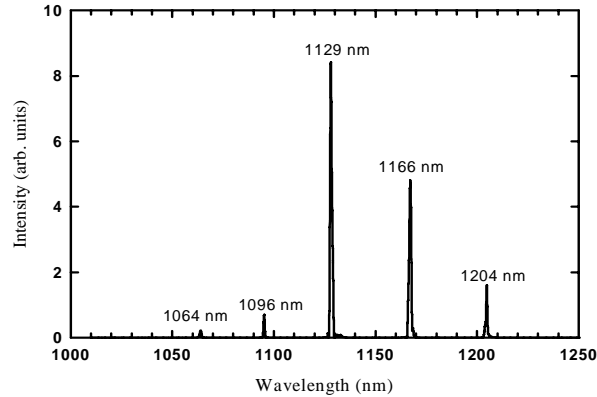


Fig. 4. Emission spectrum measured at the output of the Raman laser for the pump power of 14 W.

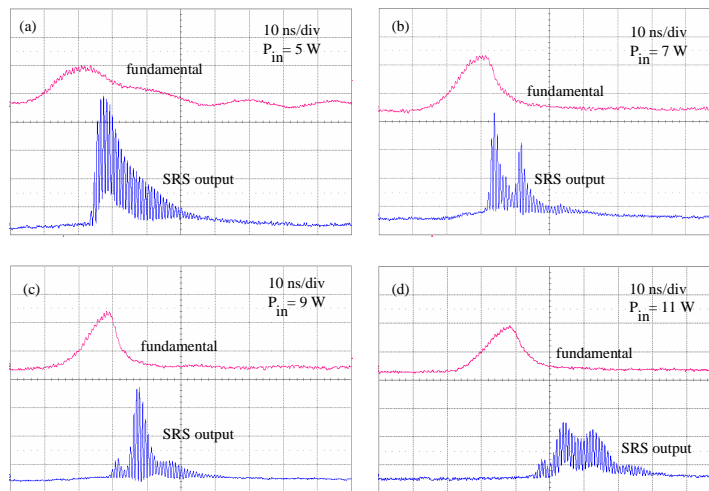


Fig. 5. Temporal characteristics of the fundamental pulse and Raman pulses (a) 5 W, (b) 7 W, (c) 9 W, (d) 14 W.

#### 4. Conclusion

In summary, we have developed a diode-pumped actively Q-switched mixed Nd:Y<sub>0.3</sub>Gd<sub>0.7</sub>VO<sub>4</sub> laser with an intracavity KTP crystal to produce cascade SRS emission up to the fourth order. With an incident pump power of 14 W and a repetition rate of 50 kHz, the average output powers at 1096 nm, 1129 nm, 1166 nm, and 1204 nm are approximately 0.05 W, 0.61 W, 0.25 W, and 0.11 W, respectively. The maximum peak power is found to be higher than 2 kW.

#### Acknowledgments

The authors also thank the National Science Council for their financial support of this research under Contract No. NSC-95-2112-M-009-041-MY2.